



Benthic diatoms modify riverine silicon export to a marine zone in a hypertidal estuarine environment

Holly Wallington · Katharine Hendry ·
Rupert Perkins · Marian Yallop · Sandra Arndt

Received: 20 September 2022 / Accepted: 16 November 2022 / Published online: 1 December 2022
© The Author(s) 2022

Abstract Riverine dissolved silicon (DSi) and biogenic silica (BSi) are modulated along the estuarine gradient by several biotic and abiotic processes governed by physical forcings. An important area controlling silicon transport in alluvial estuaries with large intertidal mudflats is the benthic diatom-dominated biofilm system. Here, the hypertidal Severn Estuary, UK, has been used as a case study to

improve our understanding of silicon transport in these benthic-dominated systems. We present the first time-series dataset of Si concentrations in the Severn. River and tidal hydrodynamics drove spatio-temporal changes in DSi. The longitudinal profile of DSi followed the classical view of dilution with downstream transport. Despite low riverine supply of BSi and low siliceous-phytoplankton production, relatively high BSi concentrations were measured in the Severn Estuary (maximum of 14.9 mg/L), which accounted for over 70% of the total bioavailable silicon present and were characterised by isotopically heavy waters ($\delta^{30}\text{Si}$ of +0.9 to +1.1‰). Benthic biofilms (microphytobenthos) on the intertidal mudflats contained significant biomass (measured as chlorophyll *a* concentration with a maximum of $116.8 \pm 16.2 \mu\text{g/g dw. sed}$) with high productivity, driven by their photo-protective adaptations to these harsh intertidal environments, contributing to isotopically heavy mudflat water ($\delta^{30}\text{Si}$ of +1.19 to +2.03‰), and resulting in high benthic BSi content in the spring ($0.74 \pm 0.03\%$) and summer ($0.76 \pm 0.05\%$). The fast-flowing tidal currents resulted in high bottom shear stress which likely exceeded the erosion thresholds of the biofilms, transporting the sediment-BSi matrix into the water column. Suspended particulate matter (SPM) and BSi remained tightly coupled in the estuarine water column (biofloculation), and experienced the series of erosion–deposition events, burial/dissolution and export out of the estuary. Our novel observations improve understanding of the complex processes

Responsible Editor: Marguerite A Xenopoulos.

Supplementary Information The online version contains supplementary material available at <https://doi.org/10.1007/s10533-022-00997-7>.

H. Wallington · K. Hendry (✉)
School of Earth Sciences, University of Bristol,
Bristol BS8 1RJ, UK
e-mail: k.hendry@bristol.ac.uk

K. Hendry
British Antarctic Survey, Natural Environment Research
Council, Cambridge CB3 0ET, UK

R. Perkins
School of Earth and Ocean Sciences, Cardiff University,
Cardiff CF10 3AT, UK

M. Yallop
School of Biological Sciences, University of Bristol,
Bristol BS8 1TQ, UK

S. Arndt
Department Geoscience, Environment & Society (DGES),
Université Libre de Bruxelles, BGeosys, Brussels,
Belgium

governing Si transport in hypertidal, benthic-dominated estuaries, and highlights the importance of tightly coupled benthic-pelagic systems in influencing the terrestrial silicon export to a marine zone.

Keywords Silicon · Biogenic silica · Severn estuary · Biofilms

Introduction

Diatoms have an obligate growth requirement for dissolved silicon (DSi). Diatoms uptake DSi and through biomineralization form their particulate silica frustules, hereafter referred to as biogenic silica (BSi). These siliceous organisms contribute up to 40% of global marine productivity, and through high BSi export rates to the deep ocean, are a critical component of the biological carbon pump (Tréguer et al. 2018, 2021).

DSi enters the hydrosphere and is transported to the ocean via rivers and groundwater (Frings et al. 2016), accounting for 70–85% of all DSi inputs into the ocean (Tréguer & De La Rocha 2013; Tréguer et al. 2021). Rivers are a key network in transporting BSi from the terrestrial environment to the marine zone (Tréguer et al. 2021). Studies into estuarine Si cycling have gained momentum with new insight into the role of the coastal ecosystem on biogeochemically modifying the riverine Si inputs to a marine zone (e.g., Arndt et al. 2007; Arndt and Regnier 2007; Patuszak et al. 2008; Carbonnel et al. 2009, 2013; Leynaert et al. 2011; Li et al. 2019; Zhang et al. 2020; Sarath et al. 2022), including the importance of estuarine benthic-pelagic coupling (e.g., Raimonet et al. 2013; Welsby et al. 2016).

Estuarine benthic ecosystems are potential areas of high biogeochemical cycling activity and are among some of the most productive ecosystems globally. Estuarine biogeochemical processes interact on different spatio-temporal scales, induced by a wide range of physical forcings (Regnier et al. 2013). As a result, pelagic DSi and BSi fractions, hereafter PDSi and PBSi, are biogeochemically modified along the estuarine gradient due to the interaction of hydrological, geochemical, and biological processes over different spatio-temporal scales. However, these coastal modifications to the terrestrial Si inputs are likely to have consequences for the coastal and marine ecosystems,

for global biogeochemical cycles, and ultimately, for the estimates of both global terrestrial and marine Si budgets (e.g., Tréguer et al. 2021). Current global Si budget estimates have considered estuarine Si cycling; however, they have primarily focused on two processes: the pelagic Si biological production and reverse weathering, neglecting the potential Si supply from the estuarine benthic ecosystem. By disregarding the potential estuarine benthic Si cycle, estimates of the Si budgets are accompanied by large uncertainties. Further, to date, estuaries and the coastal environment remain under-sampled (Brewin et al. 2016), leaving changes in the Si budgets to go unnoticed through the filter of land–ocean exchange.

Despite previous estuarine Si cycling studies, which are often centred on the Scheldt Estuary (e.g., Struyf et al. 2005a, 2005b; Arndt and Regnier 2007; Arndt et al. 2007; Carbonnel et al. 2009, 2013) Bay of Brest (e.g., Ragueneau et al. 2005), Chesapeake Bay (e.g., Conley and Malone 1992) and Yangtze (Li et al. 2019; Zhang et al. 2020), knowledge of the potential Si modifications in an estuary which is dominated by a biologically productive benthic system, are less well-known. Substantial research has been carried out on the role that saltmarshes and wetlands play in cycling Si in the coastal environment (e.g., Struyf et al. 2005a,b, 2010; Jacobs et al. 2008; Carey and Fulweiler 2014), but few have studied the complex benthic diatom-dominated biofilm ecosystem on intertidal mudflats. The role of the biofilms in biostabilizing the sediment has been extensively researched (e.g., Paterson 1989; Underwood and Paterson 1993; Sutherland et al. 1998; Stal and De Brouwer 2003; Perkins et al. 2004) but the contribution of Si to the coastal budget, is often overlooked. Here, we aim to draw attention to the importance of this neglected benthic system in modifying riverine DSi and BSi exports to a marine zone. In doing so, we also use Si isotope measurements as an exciting new approach to understand Si transport in these complex and tightly coupled benthic-pelagic systems. Only a few studies have applied Si isotopes to estuaries: the Scheldt Estuary (Delvaux et al. 2013), the Changjiang Estuary (Zhang et al. 2015), and those of the world's largest rivers: the Amazon, Yangtze and Pearl rivers (Zhang et al. 2020). Knowledge of the extent estuaries alter the isotopic Si signature prior to reaching the oceans, is therefore poorly constrained.

The Severn Estuary (UK) is a suitable case study to investigate the effect of benthic–pelagic coupling on the transport of DSi and BSi in an estuary. The Severn is heterogeneous because of complex hydrogeomorphological dynamics and has the second largest hyper-tidal range on Earth. This large tidal range results in the development of large intertidal mudflats, inhabited by diatom-dominated microphytobenthic (MPB) biofilms at the sediment–water interface (SWI) (Underwood 2010). The biofilms are subjected to high resuspension rates (Manning et al. 2010) associated with the extreme tidal dynamics (Neil and Couch 2011), creating a potential export of Si from the benthic system into the water column. Due to high turbidity in the water column (Manning et al. 2010), which limits phytoplankton growth (Underwood 2010), the photosynthetically productive diatom biofilms (Welsby et al. 2016) have a high potential to biologically mediate Si through the uptake of benthic DSi (BDSi) and through biosilicification, the production of benthic BSi (BBSi). With the potential strong benthic–pelagic coupling between the benthic ecosystem on the intertidal mudflats and the Severn’s water column, the biogeochemical forcings, alongside the estuarine hydrodynamics, are expected to significantly influence the transport of Si.

We hypothesized that a proportion of the pelagic BSi may originate from the resuspended MPB biofilms inhabiting the intertidal mudflats of the Severn Estuary. Our first aim was to investigate the effects of multiple forcings that influenced the transport and transformations of PDSi and PBSi along the Severn Estuary. These forcings were investigated by analysing the: river discharge rates; salt and sediment transport (Suspended Particulate Matter, SPM); pelagic biomass (chl *a*); Total Organic Carbon (TOC) concentrations; and macronutrient (nitrate, nitrite, ammonium, and phosphate) concentrations; and Si input from external sources including the estuarine tributaries and DSi inputs from groundwater and rainwater. Our second aim was to determine the relative importance of the benthic system of the intertidal mudflats of the Severn Estuary as a source of Si to the water column. This was addressed by determining the BDSi and BBSi budgets of the MPB biofilms inhabiting the intertidal mudflats of the Severn Estuary, using stable silicon isotopes to investigate uptake mechanisms, and by exploring the multiple factors that could influence the uptake of BDSi and the subsequent build-up

of BBSi in benthic regions over spatio-temporal scales.

Methods

Sampling methodology

Ecological surveys were carried out each season in 2016 in the River Severn, Severn Estuary and upper Bristol Channel (Fig. 1). The sampled periods coincided with the seasons, and for clarity, are referred to hereafter as; winter (January–March), spring (April–June), summer (July–September) and autumn (October–December). However, due to constraints, these sampled days, although span the entire season, do not necessarily reflect the temporal change associated with each season, which would require daily sampling. Distances along the river–estuary system were calculated using UK Ordnance Survey base-maps in ArcGIS. A transect was taken, aboard a research vessel, from the upper estuary at high tide, along the longitudinal axis, to the outer estuary. Water was collected from the surface (<2 m deep) and at depths (>15 m deep) using a 5 L Niskin bottle. A transect of four stations was taken along each of the main tributaries: River Wye, River Usk, and River Avon, along with a sampling station in Cardiff Bay (Rivers Taff and Ely). These tributaries discharge into the estuary between *ca.* 15 and 45 km from the lower estuarine boundary. Sampled intertidal mudflat sites, which coincided with spring cycles, ranged from the upper Severn Estuary at Severn Beach, Site 1 (51.57° N, 2.67° W), to the mid-estuary on the English coast at Portishead, Site 2 (51.49° N, 2.77° W), and on the Welsh coast at Newport Wetlands, Site 3 (51.53° N, 2.92° W), to the outer estuary at Sand Bay, Site 4 (51.38° N, 2.97° W).

Three replicates (3 × 1 L) of river and estuary water were sampled to measure PBSi and chlorophyll (chl) *a* concentrations from the filtered matter. Estuarine pelagic chlorophyll fluorescence was measured using the Water Pulse Amplitude Modulation (PAM) fluorometer (Walz, Effeltrich, Germany) on sub-samples of freshly collected water, using the cuvette system of the WATER-ED Emitter-Detector Unit. However, water column productivity was too low for any measurements ($F < 150$ *rel. units*). Acid cleaned (10% HCl) HDPE bottles were filled

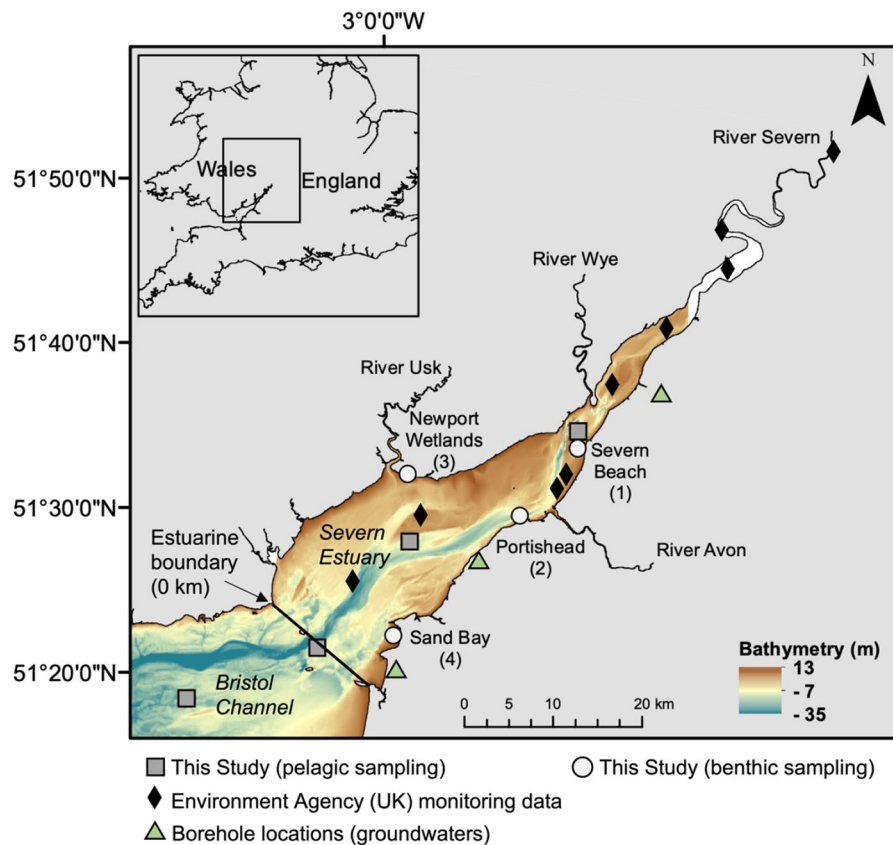


Fig. 1 The Severn Estuary is situated in the southwest of the United Kingdom between England and Wales (see inset—box shows location of A). A The River Severn (river), Severn Estuary (estuary) and Bristol Channel (marine end-member). Severn Estuary bathymetry (depth relative to OSGB 1936 datum). Pelagic sampling points (squares) in the upper, middle, and lower estuary and Bristol Channel. Sampled stations were: The shoots (~51.55° N, 2.71° W), South Middle Grounds (~51.45° N, 2.96° W), and Tail Patch (~51.37° N, 3.06° W). A station in the Bristol Channel (Culver Sands: ~51.29° N, 3.18° W) was sampled for the marine end-member silicon concentrations. Mudflat sampling sites (circles): Severn Beach (Site 1), Portishead (Site 2), Newport Wetlands (Site 3) and Sand Bay (Site 4). Environment Agency (2016) monitor-

ing sampling stations (diamonds) and borehole locations (triangles). A separate transect of four stations was sampled at low tide along the River Severn: Epney (51.78° N, 2.35° W), Elmore (51.83° N, 2.30° W), Maisemore (51.88° N, 2.27° W), Tirley (51.93° N, 2.22° W). The lower estuarine boundary which lies between Weston-super-Mare and Lavernock (marked 0 km) is the reference point for the samples. Distance of the sampled stations in the River Severn from this boundary: Tirley (112 km), Maisemore (103 km), Elmore (96 km) and Epney (83 km). Distance of the sampled stations in the Severn Estuary from this boundary: The Shoots (33 km), South Middle Grounds (14 km) and Tail Patch (5 km). Distance of the sampled station in the Bristol Channel from this boundary was Culver Sands (–10 km)

with 50 mL filtered water through PALL Acrodisc PF 32 mm syringe filters with 0.8/0.2 µm pore space supor membranes for analysis of PDSi, Total Organic Carbon (TOC), and macronutrient (nitrate, nitrite, ammonium, and phosphate) concentrations, along with Si isotopes. Three water sample replicates (3 × 1 L) were collected for suspended particulate matter (SPM) concentrations (g/L). River water pH was logged using pH-Pal-Pocket testing (ETI

Instruments, U.K.) calibrated to a pH buffer of 4, 7 and 10. Riverine conductivity was measured using a conductivity probe calibrated using potassium chloride, and converted to salinity (PSU). Air and water temperatures were recorded using a hand-held thermometer.

Microphytobenthic biofilms at the SWI were sampled during daytime low tide periods, between ~11:00 h and 16:00 h. At each mudflat, 15

replicates were taken, along a ~100 m transect, at the mid-shore tide height, parallel to the surf zone, using a semi-random sampling scheme targeting areas of extensive biofilms, with ~5 m between each sample of biofilm. Three field replicates were taken at each station to capture the natural variability of the system on the metre scale. Sediment mini-cores of a diameter of 2.5 cm were extracted for the surficial 5 mm biofilm for chl *a* analysis and BBSi content. Variable chlorophyll fluorescence of undisturbed diatom-dominated biofilms was logged at each station as a proxy for photosynthesis (see Online Resource 1). A sample (50 mL) of the mixed mudflat water (a mixture of surface and pore fluids) was placed into acid (10% HCl) cleaned 50 mL centrifuge tubes, centrifuged at 4000 rpm for 10 min, with the supernatant decanted and filtered through PALL Acrodisc PF 32 mm syringe filters with 0.8/0.2 µm pore space supor membranes for the concentrations of BDSi, phosphate, nitrate, nitrite, ammonium and total organic carbon (TOC).

Sediment porosity (ϕ) (Eq. 1) was calculated at each station, as a function of the wet and dry sediment mass, and the wet bulk density ρ_s (assumed to be 1.5 for unconsolidated sediment), and the density of water ρ_w (assumed to be that of seawater, 1.02).

$$\phi = \frac{[\text{Mass of wet sediment (g)} - \text{mass of dry sediment (g)}]}{\text{mass of wet sediment (g)} \times \rho_s / \rho_w} \quad (1)$$

Rainwater was collected in the vicinity of the Severn Estuary, once a month (max. 12 h), for 4 months, in 2016 using a pre-cleaned 1L plastic bottle. Groundwater data from boreholes were obtained from the Environment Agency (EA), UK, a national organisation that collects environmental monitoring data. Sunshine hours were from the UK Met Office (Met Office, 2016), and, at each station, ambient irradiance (mmol photons/m²/s) was measured using the Mini Quantum Sensor attached to the Walz PAM fluorometer.

Tidal velocities were compared to the bottom shear stress to assess erosion capacity. Bottom shear stress (τ_b in N/m²) was determined by the quadratic friction law (Eq. 2):

$$\tau_b = \frac{\rho * g |V|V}{C^2} \quad (2)$$

where, ρ is the density of pure water (1000 kg/m³), g is the acceleration due to gravity (m/s²), V is the tidal current velocity in the estuary (m/s), and C is the Chézy coefficient, with typical values of 40 m^{1/2}/s for estuaries (Volta et al. 2014).

Laboratory analysis

Approximately 25% of the surficial biofilms were removed from the mudflat sediment mini-cores and dried in an oven at 85 °C for 24 h to determine the percentage loss of weight upon drying. Benthic and pelagic samples (~0.05 g) were measured for BSi using the weak alkaline extraction method adapted from DeMaster (1981). BSi concentrations were measured using the standard Heteropoly Blue method, modified from the original molybdate acid spectrophotographic method on a Hach Lange DR3900 spectrophotometer (Strickland and Parsons 1972). Blanks were processed alongside each sample. The internal error of the spectrophotometer was 2%.

Chl *a* content was used as a proxy for biofilm and water column photosynthetic biomass and was determined following Mackereth et al. (1978). Briefly, the chl *a* from the filters or the sediments were extracted for 24 h using 4 mL acetone buffered with MgCO₃ to prevent degradation of chl *a* to phaeophytin, with samples kept in the dark at 4 °C. The samples were then centrifuged at 2000 rpm for 15 min, and then analysed in a JENWAY 6305 spectrophotometer (absorbances at 630 nm, 647 nm, 664 nm, and 750 nm). Chl *a* was then calculated using the optical densities at the different wavelengths corrected for scattering at 750 nm (Eq. 3).

$$\text{Chla} = 11.85 \times \text{OD}_{664} - 1.54 \times \text{OD}_{647} - 0.08 \times \text{OD}_{630} \quad (3)$$

Aliquots of all filtered mudflat and river waters (200 µL) were diluted with Milli-Q H₂O (9.8 mL) for DSi concentration analysis (mg/L) following the Heteropoly Blue method (Strickland and Parsons 1972). Sub-samples (2.0 mL) were measured for phosphate concentrations (PO₄-P, mg/L), following the LCK 349 method. All phosphate concentrations were below 50 mg/L and did not interfere with the BSi measurements. Nitrate (NO₃-N) and nitrite (NO₂-N) concentrations (mg/L) were measured from sub-samples (2.0 mL) using the LCK method

339 and 341, respectively. Ammonium concentrations ($\text{NH}_4\text{-N}$, mg/L) were measured from subsamples (5 mL) using the 304 LCK method. Due to interferences of chloride ions on these macronutrients, HDPE bottled estuarine water samples were immediately frozen and were analysed for PDSi and other macronutrient concentrations (mg/L) on a SEAL analytical AIII segmented flow colorimetric auto-analyser at Plymouth Marine Laboratory following the methodology recommended by GO-SHIP (Hydes et al. 2010). TOC concentrations were measured using the Non-Purgeable Organic Carbon (NPOC) technique (Visco et al. 2005) at the School of Geographical Sciences, University of Bristol.

Filtered pelagic and benthic mudflat water from the summer and autumn sampled periods of 2016 were analysed for their Si isotope value (presented here as $\delta^{30}\text{Si}$, see Eq. 4). Saline water samples were prepared following the MAGnesium Induced Co-precipitation (MAGIC) method using sodium hydroxide (Karl and Tien 1992) with (Reynolds et al. 2006) modifications, prior to column chromatography, using the cation exchange resin, adapted from George et al. (2006). The BioRad resin (DOWEX 50 W-X12, 200–400 mesh) was pre-cleaned, and rinsed with acid (3 M, 6 M and concentrated HCl) and MQ, before the sample and standards were passed through the columns. The determination of Si isotopes (^{28}Si , ^{29}Si , ^{30}Si) was performed on a Thermo Scientific Neptune Plus High Resolution multicollector inductively coupled plasma mass spectrometer (MC-ICP-MS) at the Bristol Isotope Group laboratories. Raw measurements were blank corrected and corrected for instrument mass bias which affects fractionation, using a standard-sample bracketing protocol and Mg isotope correction (Cardinal et al. 2003). The standards and samples have ^{29}Si and ^{30}Si values that fall along the expected mass-dependent fractionation line, with ^{30}Si : $^{29}\text{Si} = 0.512^{30}\text{Si} \pm 0.04$, $r^2 = 0.997$, $n = 42$, which fall between the mass-dependent relationship for kinetic and equilibrium fractionation (Georg et al. 2006). The long-term external reproducibility of the measurements was assessed using the sponge standard LMG08 (Hendry et al. 2011), with values measured at: $\delta^{29}\text{Si} = -1.71 \pm 0.07\text{‰}$ and $\delta^{30}\text{Si} = -3.47 \pm 0.06\text{‰}$, $n = 17$. These values compared well to reported mean values (Hendry et al. 2011) of: $\delta^{29}\text{Si} = -1.72 \pm 0.08\text{‰}$, and

$\delta^{30}\text{Si} = -3.37 \pm 0.17\text{‰}$. Full replicate $\delta^{30}\text{Si}$ measurements of river samples agreed within $\pm 0.08\text{‰}$ or better.

$$\delta^{30}\text{Si} = \left(\frac{\left(\frac{x_{\text{Si}}}{^{28}\text{Si}} \right)_{\text{SMP}}}{\left(\frac{x_{\text{Si}}}{^{28}\text{Si}} \right)_{\text{STD}}} - 1 \right) \times 1000 \quad (4)$$

where, x corresponds to ^{29}Si or ^{30}Si , SMP is the sample, and STD is the standard Quartz RM8546 (NBS-28).

Statistical analysis

Data was tested for normal distribution ($p > 0.05$) and equal variance ($p > 0.05$). Data that met these assumptions were tested using Two-Way ANOVA (spatial and temporal difference). However, when the Two-Way ANOVA showed significant interaction, data was tested using One-Way ANOVA, followed by a post hoc test. Data which failed to meet the assumptions of normal distribution were log transformed. Data that failed to meet the assumptions of both normality and equal variance were tested using the non-parametric Kruskal–Wallis test, followed by a post hoc Mann–Whitney pairwise test. To test the linear associations between Si and biological, nutrient, and environmental factors in the benthic and pelagic systems, Pearson's product momentum correlations were applied. A Principal Component Analysis (PCA) was applied to normalized data to assess the interaction between Si and biological, nutrient and environmental factors in the pelagic and benthic systems. The Environment Agency's (EA 2016) monitoring data has been used to validate the data presented here.

Results

Silicon transport along the Severn river-estuary-marine continuum

PDSi concentrations (mg/L) (Fig. 2) progressively decreased along the estuarine salinity gradient. Despite the temporal difference between the data presented here and the Environment Agency's monitoring data (EA 2016), a similar PDSi profile was found along the Severn (Fig. 2). PBSi concentrations

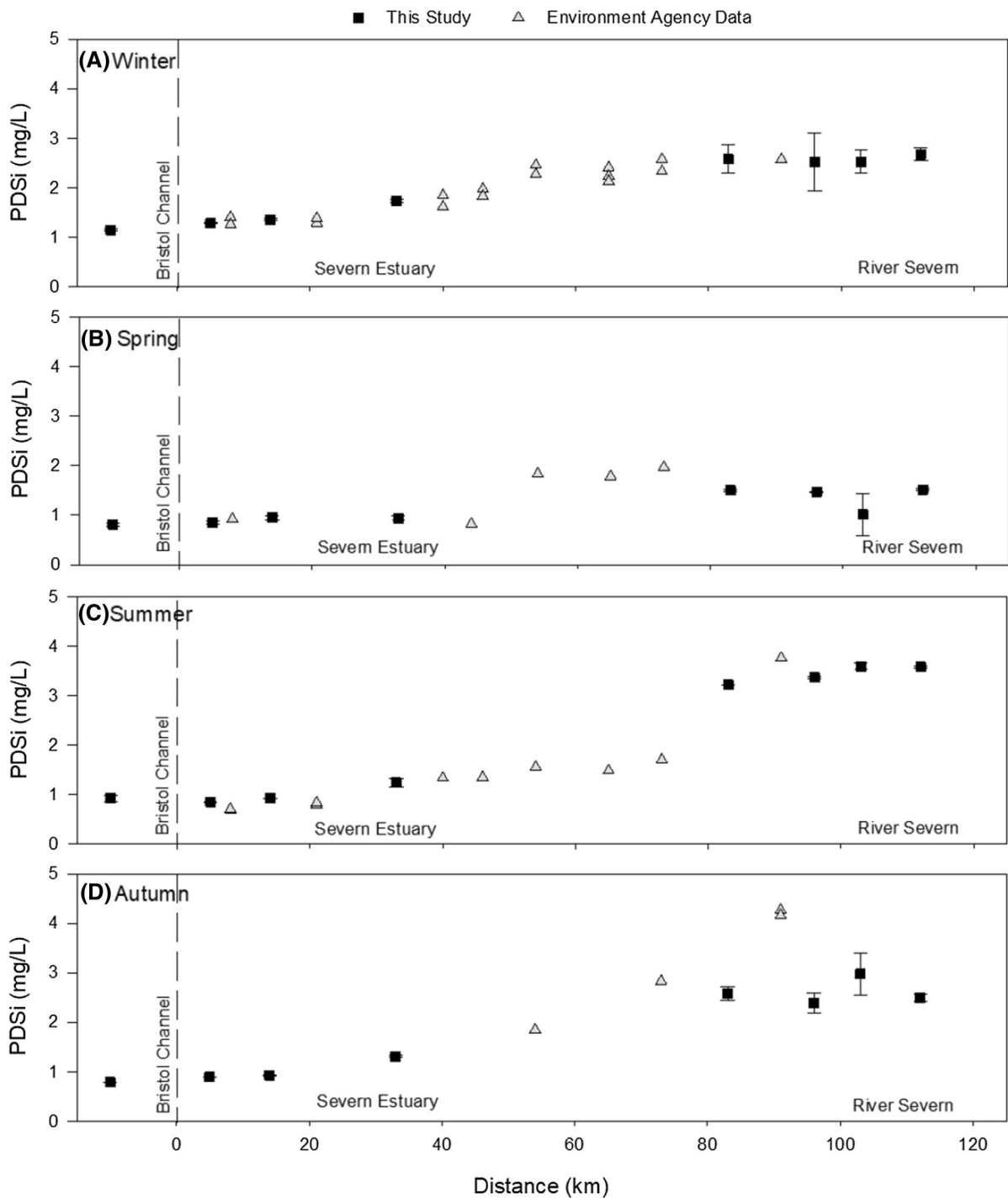


Fig. 2 Pelagic silicon concentrations along the Severn each season in 2016. This study (black squares). Environment Agency data 2016 (grey triangles). **A** Winter. **B** Spring. **C** Summer. **D** Autumn. River Severn: 80–120 km. River-Estuary

transition zone: 40–80 km (no data available). Severn Estuary: 0–40 km. Lower estuarine boundary defined as 0 km. Upper Bristol Channel: <0 km. Data reported with 1SE for each station: river ($n=3$), estuary ($n=6$)

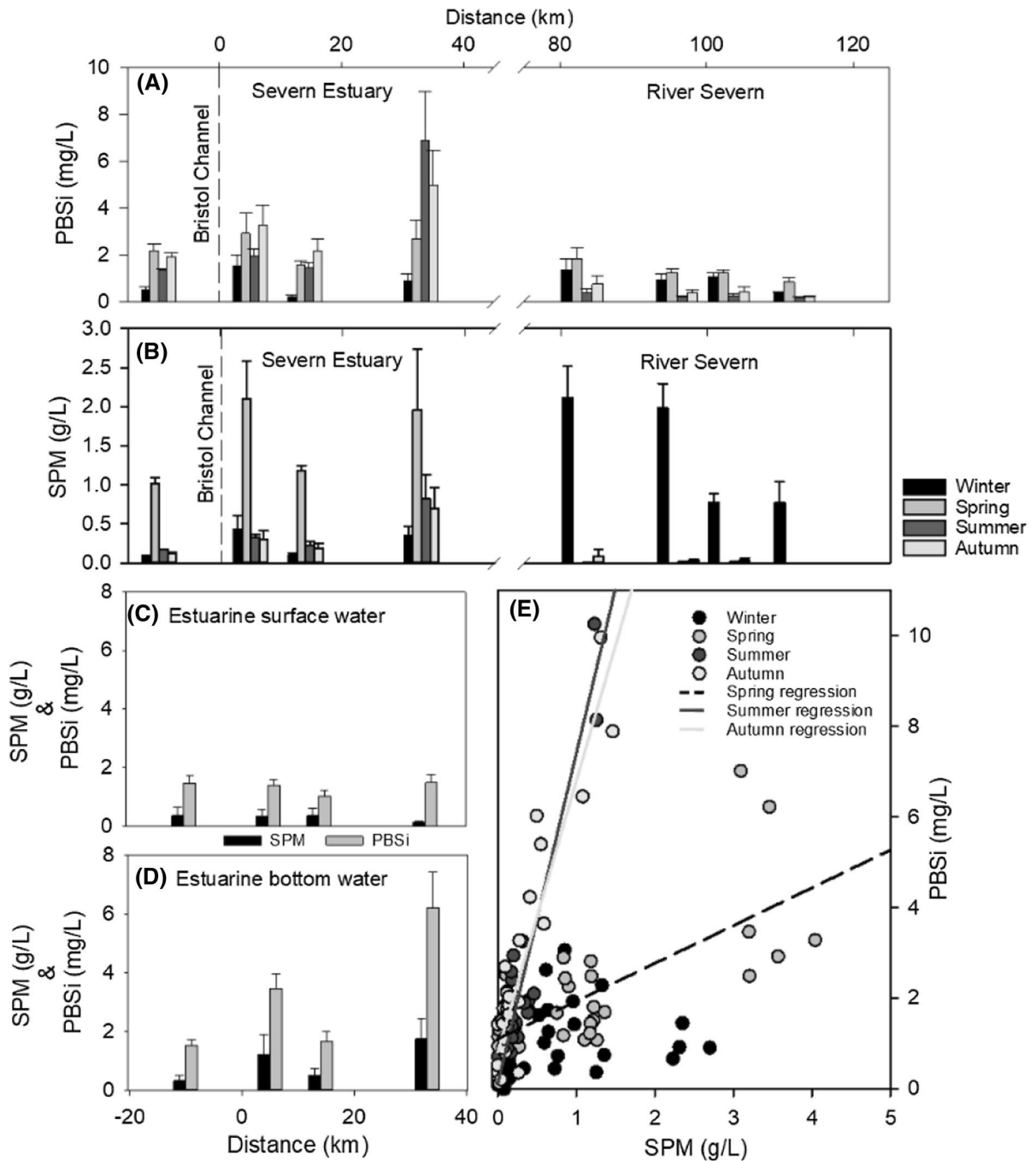


Fig. 3 **A** Pelagic BSi concentrations along the Severn each season in 2016. River Severn: 80–120 km. River-Estuary transition zone: 40–80 km (no data available). Severn Estuary: 0–40 km. Lower estuarine boundary defined as 0 km. Upper Bristol Channel: < 0 km. Data reported with 1SE for each station: river ($n=3$), estuary ($n=6$). **B** SPM concentrations (g/L) in the Severn during sampled period of 2016. Data reported with 1SE for each station: river ($n=3$), estuary ($n=6$). **C**

Estuarine surface water (< 2 m) suspended particulate matter (SPM) and pelagic biogenic silica (PBSi) concentrations, presented with 1SE ($n=12$). **D** Estuarine bottom water (> 15 m) average SPM and PBSi concentrations, presented with 1SE ($n=12$). Note, unit discrepancy: SPM (g/L), PBSi (mg/L). **E** Linear correlation between PBSi and SPM in the Severn: spring ($n=36$, $r^2=0.52$, $p<0.01$) summer ($n=36$, $r^2=0.84$, $p<0.001$) and autumn ($n=36$, $r^2=0.86$, $p<0.001$)

lacked a specific trend along the Severn (Fig. 3). Relatively higher PBSi concentrations were measured in the estuary each season compared to the river and marine zone. Peak PBSi concentrations were observed in the upper estuary in the summer and autumn sampled periods (max. 14.9 mg/L and 10.0 mg/L, respectively). PBSi concentrations displayed significant variation between sampling periods ($H=20.35$, $d.f=3$, $p<0.001$). A significant difference was found between the winter and the other sampled periods (post hoc analysis $p<0.05$), but no difference was found between samples analysed in the spring, summer and autumn periods. No linear correlation was observed between PDSi and PBSi in the Severn. PDSi dominated 76% of the proportion of Si (PDSi+PBSi) in the River Severn, whereas in the estuary BSi dominated, especially in more typically biologically productive periods: spring (72%), summer (77%) and autumn (77%), compared to the winter (38%) (Table 1).

Factors that influenced PDSi and PBSi transport in the Severn

Estuarine tributaries (River Wye, Usk and Avon)

PDSi concentrations in the tributaries (min. 0.2 mg/L, max. 5.7 mg/L) were comparable to the PDSi concentrations measured in the River Severn (min. 0.2 mg/L, max. 3.8 mg/L) (see Online Resource 2). Environment Agency (EA 2016) monitoring PDSi data for

Table 1 Proportion of PDSi and PBSi compared to the total amount of bioavailable Si (PDSi+PBSi) in each sampled period

Season	Location	PDSi (%)	PBSi (%)
Winter	River	73	27
Spring		52	48
Summer		93	7
Autumn		85	15
Winter	Estuary	62	38
Spring		28	72
Summer		23	77
Autumn		23	77
2016	River	77	23
2016	Estuary	30	70

PBSi dominated the available Si in the typically more biologically productive periods (in bold)

the Avon at Keynsham in 2016 were in a similar range between 1.2 and 5.6 mg/L. PBSi concentrations in the tributaries were higher with a wider range (min. 0.0 mg/L, max. 19.4 mg/L, avg. 1.9 ± 0.9 mg/L) compared to PBSi concentrations measured in the River Severn (min. 0.1 mg/L, max. 2.5 mg/L). However, the highest PBSi concentrations of 19.4 mg/L were recorded in the River Usk ~12 km upstream of the river mouth, with a visible tidal influence: high salinity levels of 10 PSU and high SPM concentrations of up to 2.6 g/L.

Rainwater and groundwater supply of DSi

DSi concentrations in the rainwater remained below 0.3 mg/L. Environment Agency groundwater DSi concentrations data from boreholes in the southwest UK in the catchment area for the Severn Estuary (Fig. 1), ranged between 6.7 and 9.9 mg/L (Environment Agency 2017).

Biological mediation of silicon: pelagic productivity

Water column biomass concentrations (chl *a* in mg/L) were negligible in all sampled periods in the turbid Severn Estuary and Bristol Channel (Fig. 3) and remained below 0.001 mg/L in the river. Similarly, Environment Agency monitoring chl *a* data was also low in the Severn (avg. 0.003 mg/L), with relatively higher concentrations in the river compared to the estuary. Total Organic Carbon (TOC) concentrations in the River Severn were between the limit of detection and 4.5 mg/L but lacked significant correlation with PBSi in all seasons.

Turbidity was high with low secchi disk depths in winter (0.18 m), spring (0.15 m), summer (0.2 m), and autumn (0.3 m). Significantly higher ($H=17.286$, $d.f=3$, $p<0.001$, post hoc analysis $p<0.05$) riverine SPM concentrations were measured during the winter (max. 2.1 g/L), compared to the spring (where concentration were always below the limit of detection), summer (max. 0.01 g/L) and autumn (max. 0.08 g/L). In the tidally dominated Severn Estuary, seasonal changes in river flow rates had less of an influence on the estuarine turbidity, with high SPM concentrations, predominantly a composition of mud/clay in the upper Severn Estuary (Fig. 3). Environment Agency (EA 2016) monitoring SPM data also displayed peak SPM concentrations in the upper Severn

Estuary, and followed a similar seasonal pattern to our data: 1.1 g/L (winter), 3.2 g/L (spring), 1.5 g/L (summer), and 1.7 g/L (autumn) (Fig. 3). No clear correlation was observed between SPM and PBSi during the winter, but a positive linear correlation was observed in the more typical biologically productive periods: spring ($n=36$, $r^2=0.52$, $p<0.01$), summer ($n=36$, $r^2=0.84$, $p<0.001$) and autumn ($n=36$, $r^2=0.86$, $p<0.001$) (Fig. 3). Bottom water samples in the Severn Estuary had higher concentrations of SPM and PBSi compared to surface water samples each sampled period in 2016 (Fig. 3).

Macronutrient concentrations were high in the River Severn compared to the Severn Estuary and Bristol Channel, similar to a decrease in DSi at higher salinity levels (Table 2). In each sampling period, nitrate was the most abundant macronutrient in the River Severn (annual avg. of 4.4 ± 0.7 mg/L) and the Severn Estuary (annual avg. of 1.5 ± 0.3 mg/L) and displayed greater temporal variation in the river compared to the more saline end-member. Environment Agency's (EA 2016) monitoring nitrate data were also similar with a range between 0.6 and

8.2 mg/L. Following Redfield-Brzezinski nutrient ratios of C:Si:N:P of 106:15:16:1, PDSi was potentially limiting relative to nitrate during typically biologically productive periods in the river and estuary (see Online Resource 3). Water column temperatures in the Severn were relatively lower during the winter (5.4 ± 0.3 °C) and autumn (9.3 ± 0.03 °C) compared to the spring (13.2 ± 0.1 °C) and summer (17.9 ± 0.03 °C) (Table 2). In the Severn Estuary, pH fluctuated within the range of 6.9 and 7.9. In the River Severn, pH fluctuated between 6.7 and 8.3 (Table 2).

To assess the interconnections between Si and environmental variables in the water column of the Severn, PCAs were undertaken for each sampling period in 2016 (Fig. 4). PC1 and PC2 accounted for most of the variance in the winter (71.8%), spring (71.6%), summer (87.2%), and autumn (87.7%). In the spring, summer, and autumn, PBSi clustered with SPM with high loadings.

Table 2 Pelagic environmental variables in the River Severn-estuary-marine zone each season in 2016: nitrate, phosphate, Total Organic Carbon (TOC), salinity, pH and water temperature

Season	Nitrate (mg/L)	Phosphate (mg/L)	TOC (mg/L)	Salinity (psu)	pH (range)	Water temperature (°C)
River Severn						
Winter	2.5 ± 0.2	0.32 ± 0.1	3.2 ± 0.1	0.4 ± 0.02	6.6–8.3	4.1 ± 0.4
Spring	5.6 ± 0.5	0.19 ± 0.04	3.0 ± 0.3	0.4 ± 0.01	6.7–7.8	12.8 ± 0.1
Summer	4.5 ± 0.0	0.10 ± 0.00	3.1 ± 0.1	0.2 ± 0.00	6.8–7.4	20.3 ± 0.1
Autumn	5.1 ± 0.3	0.40 ± 0.03	3.8 ± 0.1	0.3 ± 0.00	6.7–7.6	11.1*
Severn Estuary						
Winter	1.8 ± 0.1	<0.05	–	19.1 ± 0.6	7.7–7.9	6.7 ± 0.04
Spring	1.5 ± 0.1	<0.05	–	24.4 ± 0.3	7.7–7.7	13.6 ± 0.1
Summer	1.2 ± 0.1	<0.05	–	27.7 ± 0.2	6.7–7.4	15.4 ± 0.1
Autumn	1.5 ± 0.1	<0.05	–	26.9 ± 0.5	7.6–7.6	7.3 ± 0.1
Bristol Channel						
Winter	1.2 ± 0.03	<0.05	–	23.4 ± 0.00	6.9–7.9	7.0 ± 0.00
Spring	1.3 ± 0.04	<0.05	–	26.5 ± 0.00	6.7–7.7	13.1 ± 0.00
Summer	1.1 ± 0.10	<0.05	–	28.9 ± 0.00	6.7–7.5	15.8 ± 0.00
Autumn	1.0 ± 0.00	<0.05	–	29.4 ± 0.00	6.8–7.6	8.2 ± 0.00

All pelagic concentrations of nitrite and ammonium were under the level of detection (<0.15 mg/L)

Environment Agency monitoring data (EA 2016) for nitrite, phosphate and ammonium along the Severn were also of low concentration: nitrite (0.004–0.1 mg/L), phosphate (0.05–0.4 mg/L), ammonium (0.02–0.1 mg/L)

*refers to thermometer readings where the triplicate measurements agreed within error (0.1 °C)

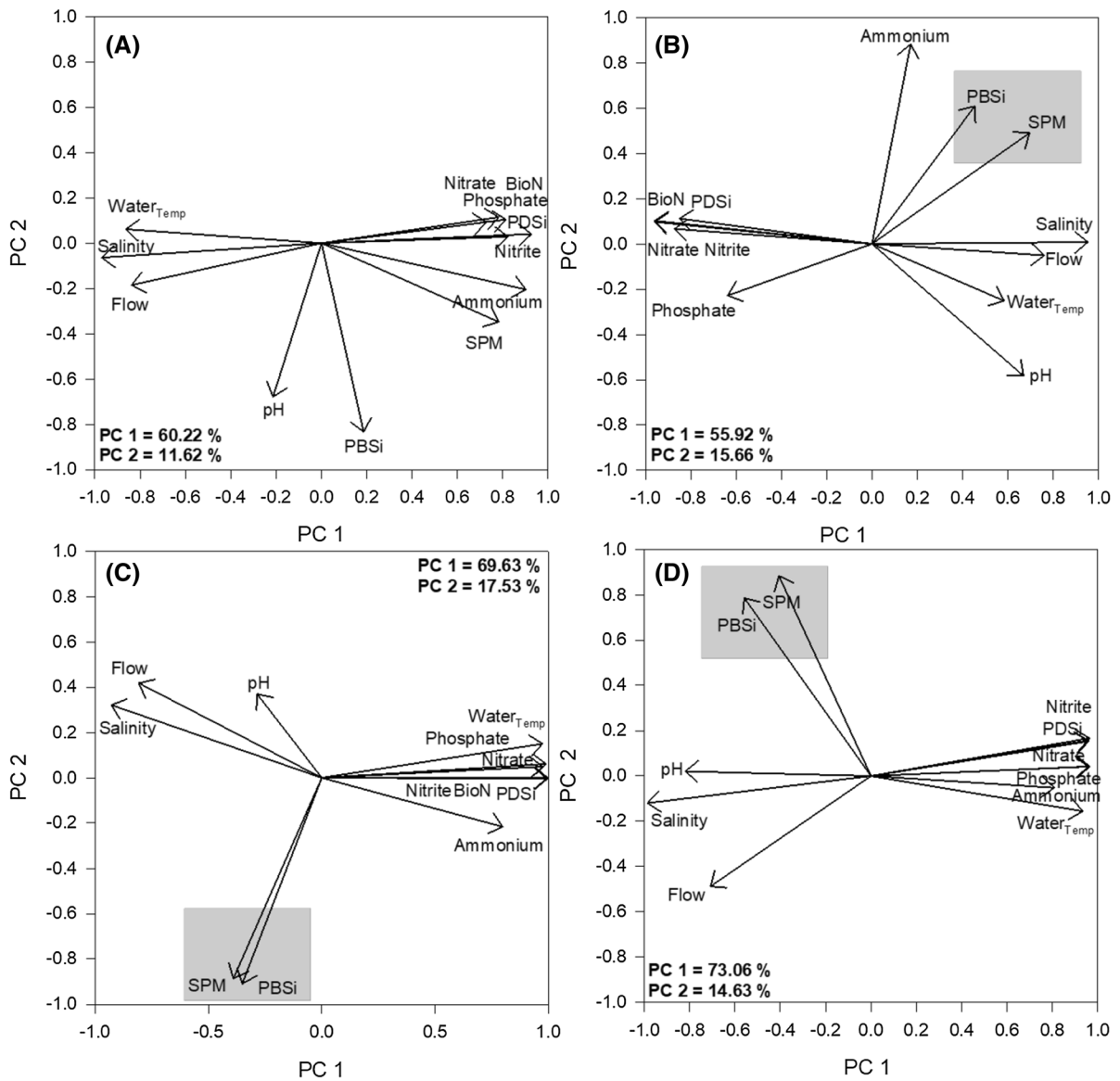


Fig. 4 Principal Component Analysis: PC1 vs PC2 loadings plots for the interconnections between pelagic dissolved silicon (PDSi), pelagic biogenic silica (PBSi) and environmental vari-

ables in the water column of the Severn. **A** Winter. **B** Spring. **C** Summer. **D** Autumn

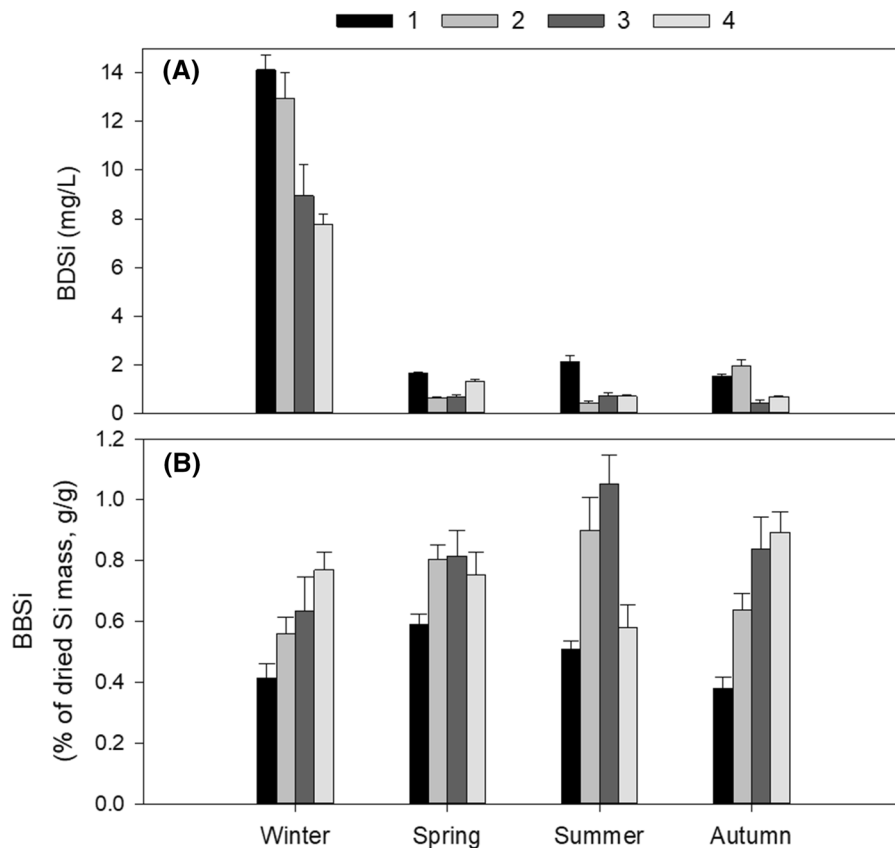
Biological mediation of silicon: benthic productivity

To determine whether the benthic Si export may have contributed to the high estuarine BSi concentrations, the benthic DSi (BDSi) and benthic BSi (BBSi) budgets on the intertidal mudflats were assessed. Porewater BDSi concentrations at all four mudflat sites averaged 10.9 ± 1.5 mg/L during the winter, and were significantly higher ($H=9.78$, $d.f=3$, $p < 0.001$)

compared to the spring (1.1 ± 0.3 mg/L), summer (1.0 ± 0.4 mg/L) and autumn (1.2 ± 0.4 mg/L) (Fig. 5). BBSi was significantly higher ($H=9.78$, $d.f=3$, $p < 0.05$) in the spring ($0.74 \pm 0.03\%$) and summer ($0.76 \pm 0.05\%$) compared to the winter ($0.59 \pm 0.04\%$) and autumn ($0.69 \pm 0.04\%$) (Fig. 5).

To interpret the spatio-temporal variability in these BDSi and BBSi budgets (Fig. 5), the combined impact of multiple consumption/production processes

Fig. 5 **A** Benthic dissolved silicon concentrations (BDSi, mg/L) from the Severn Estuary intertidal mudflat water. **B** Benthic biogenic silica (BBSi, % of dried Si mass, g/g). Sites: Severn Beach (1), Portishead (2), Newport Wetlands (3), Sand Bay (4). Presented with 1SE ($n = 15$)



were considered, with an emphasis on the benthic biological mediation of Si alongside environmental forcings. Relatively lower chl *a* content was measured during the winter ($30.6 \pm 5.0 \mu\text{g/g dw. sed.}$) and increased during the spring ($35.7 \pm 3.9 \mu\text{g/g dw. sed.}$) and summer ($55.1 \pm 6.9 \mu\text{g/g dw. sed.}$) reaching significantly higher levels ($H = 55.82$, $d.f = 3$, $p < 0.05$; post hoc analysis $p < 0.01$) during the autumn ($116.8 \pm 16.2 \mu\text{g/g dw. sed.}$) (Table 3). No significant linear correlations were calculated between BBSi and chl *a*. TOC concentrations on the mudflats ranged between 0.4 and 28.1 mg/L in the sampling periods of 2016, with a significant difference between sampled sites ($H = 25.08$, $d.f = 3$, $p < 0.001$, post hoc analysis $p < 0.001$) (Table 3). No significant linear correlations were calculated between BBSi and TOC.

Benthic biofilms during the spring and summer sampling periods were exposed to higher air and water temperatures (Table 3). Despite meteorological seasonal changes, water content in the mudflats lacked significant variability between sampling

periods: winter ($41 \pm 0.02\%$), spring ($53 \pm 0.02\%$), summer ($43 \pm 0.02\%$), and autumn ($45 \pm 0.02\%$). Sediment porosity lacked seasonal variation, with fine sediment fractions ($< 63 \mu\text{m}$) dominating the intertidal mudflats. The total number of sunshine hours were on average higher in the spring (177 h) and summer (154 h) compared to the winter (65 h) and autumn (84 h). Irradiance levels at the time of sampling were relatively high ($> 1253 \mu\text{mol photons/m}^2/\text{s}$) during the summer, and relatively lower ($< 150 \mu\text{mol photons/m}^2/\text{s}$) during the autumn and winter. The MPB biofilms were dominated by photosynthetically productive pennate diatoms, adapted to the mudflat environment (see Online Resource 1). Rapid Light Curves (used to explore the relationship between irradiance and photosynthesis) from the winter and autumn sampled periods saturated, with maximum relative Electron Transport Rates averaging $126 \pm 7 \text{ rel. units}$ in the winter and $142 \pm 28 \text{ rel. units}$ in the autumn. In contrast, the majority of RLCs from the spring and summer failed to saturate. In addition to light stress, the

Table 3 Benthic environmental variables in the Severn Estuary intertidal mudflats each season in 2016: biofilm biomass (chlorophyll *a*), relative maximum Electron Transport Rate (rETR_{max}), Total Organic Carbon (TOC), nitrate, nitrite, ammonium, phosphate, water content, air and water temperature

Season	Location	Chl <i>a</i> ($\mu\text{g/g dw.}$ sed.)	rETR _{max} (rel. units)	TOC (mg/L)	Nitrate (mg/L)	Nitrite (mg/L)	Ammonium (mg/L)	Phosphate (mg/L)	Water Content (%)	Temperature (°C)	
										Air	Water
Winter	Site 1	8±1	152±10	3.9±0.2	0.5±0.03	<LOD	0.15±0.03	0.1±0.00	41±0.01	8.0±0.1	–
	Site 2	16±4	121±22	7.5±1.9	0.4±0.04	<LOD	<LOD	0.03±0.00	34±0.00	6.8±0.1	–
	Site 3	27±13	144±14	14.5±3.0	0.4±0.03	<LOD	<LOD	0.1±0.00	43±0.05	8.2±0.1	–
	Site 4	71±8	161±20	2.7±0.1	0.5±0.02	<LOD	<LOD	0.1±0.00	45±0.01	11.8±0.2	–
Spring	Site 1	13±2	562±60	No sample	0.7±0.03	<LOD	<LOD	0.2±0.00	51±0.01	18.2±0.2	19.6±0.3
	Site 2	33±4	368±28	2.0±0.3	0.4±0.16	<LOD	<LOD	0.05±0.00	45±0.02	19.1±0.1	20.1±0.5
	Site 3	58±12	188±7	5.0±0.5	0.2±0.01	<LOD	<LOD	0.2±0.10	60±0.03	14.2±0.5	16.6±0.3
	Site 4	38±4	214±10	3.4±0.2	0.3±0.01	<LOD	<LOD	0.1±0.00	54±0.01	19.3±0.4	14.2±0.5
Summer	Site 1	86±17	446±18	5.7±0.5	0.4±0.02	<LOD	<LOD	0.1±0.00	46±0.01	20.2±0.4	22.3±0.4
	Site 2	49±5	368±30	4.8±0.3	0.3±0.02	<LOD	<LOD	0.1±0.00	46±0.02	19.6±0.3	22.3±0.3
	Site 3	75±15	351±47	3.4±0.3	0.3±0.02	<LOD	<LOD	0.1±0.00	40±0.05	20.6±0.7	22.9±0.5
	Site 4	11±3	368±29	5.5±0.2	0.2±0.01	<LOD	<LOD	0.1±0.00	40±0.01	20.7±0.4	21.8±0.5
Autumn	Site 1	26±3	222±65	4.5±0.2	0.3±0.02	<LOD	<LOD	0.1±0.00	46±0.01	18.9±0.2	17.0±0.2
	Site 2	155±51	134±8	4.3±0.2	<LOD	<LOD	<LOD	0.1±0.00	47±0.02	14.9±0.4	14.8±0.1
	Site 3	174±25	113±10	3.7±0.1	0.1±0.01	<LOD	<LOD	0.1±0.00	40±0.05	16.4±0.5	17.3±0.5
	Site 4	107±16	101±4	3.9±0.2	0.1±0.01	<LOD	<LOD	0.1±0.01	48±0.01	11.1±0.2	11.7±0.05

LOD refers to Limit of Detection (<0.1 mg/L for nitrate; <0.015 mg/L for nitrite and ammonium)

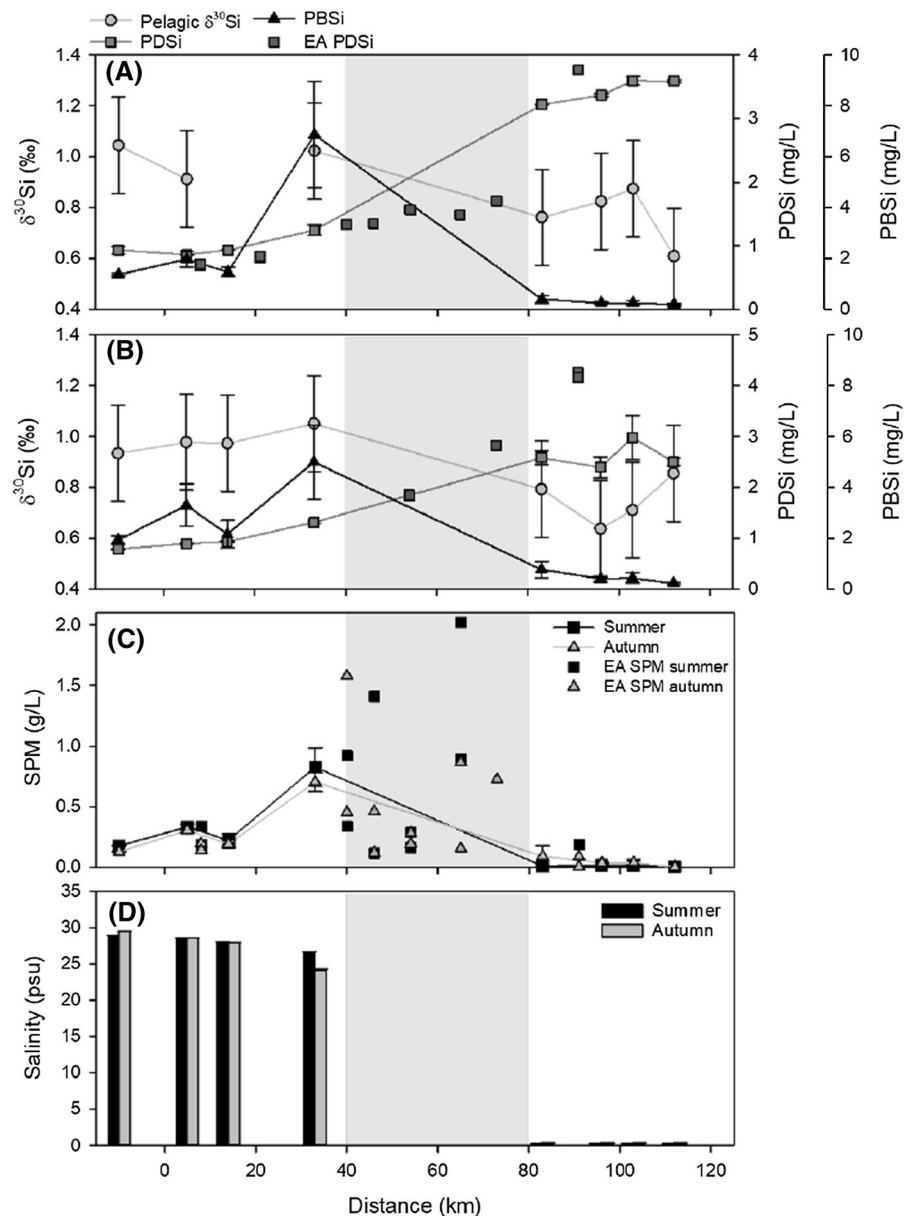
pennate diatoms experienced nutrient limitation (Table 3), in particular nitrate and DSi limitation (see Online Resource 3).

Silicon isotopes in the Severn

Pelagic $\delta^{30}\text{Si}_{\text{DSi}}$ in the summer ranged between +0.64 and +1.04‰ and between +0.63 and +1.08‰ in the autumn (Fig. 6; Online Resource 4). Estuarine waters were isotopically heavier, with $\delta^{30}\text{Si}_{\text{DSi}}$ deviating from the theoretical conservative dilution line,

indicating non-conservative behaviour between the freshwater and saline end-members. Between 40 and 80 km, considered here as the river-estuary transition zone, $\delta^{30}\text{Si}_{\text{DSi}}$ increased, corresponding to a rise in PBSi and SPM concentrations (Fig. 3). $\delta^{30}\text{Si}_{\text{DSi}}$ displayed an exponential relationship with both PBSi and SPM (see Online Resource 5). The external input of DSi with an isotopically heavy signature may have originated from the intertidal mudflats of the Severn Estuary. Studies on the Si isotopic signatures on mudflats has only recently begun, with few methodologies

Fig. 6 Silicon isotope evolution in the River Severn-estuary-marine zone. **A** Summer $\delta^{30}\text{Si}_{\text{DSi}}$. **B** Autumn $\delta^{30}\text{Si}_{\text{DSi}}$. $\delta^{30}\text{Si}_{\text{DSi}}$ presented with a LMG 2SD of 0.19. PDSi concentrations (mg/L) (grey squares) and PBSi concentrations (mg/L) (black triangles) presented with 1SE ($n=6$ per station). Pelagic $\delta^{30}\text{Si}_{\text{DSi}}$ (grey circle) presented with 2SD of long-term reproducibility. **C** SPM concentrations (mg/L) presented with 1SE ($n=6$ per station). **D** Salinity (psu), presented with 1SE ($n=6$ per station). Environment Agency monitoring data (2016) presented to fill in the transition zone where no data was collected in the present study



established to handle the high background matrix (e.g., Hughes et al., 2011), which result in significant challenges during analysis by MC-ICP-MS. The mudflat water samples analysed were characterised by high $\delta^{30}\text{Si}_{\text{DSi}}$ values (up to +2.03‰ in summer). To our knowledge, these are the first $\delta^{30}\text{Si}_{\text{DSi}}$ values from the River Severn, estuary and intertidal mudflats.

Discussion

Pelagic DSi dynamics

The high river discharge and strong tidal hydrodynamics were likely key drivers influencing the spatial variation in the transport and biological consumption of DSi and other dissolved macronutrients, with their longitudinal profiles following the classical view of downstream transport and dilution in estuaries (Chou et al. 2007) (Fig. 2). Changes in external forcing drove temporal variations in PDSi, with high rainfall and consequently high discharge rates supplying DSi to the system. This enhanced the residual downstream transport, shifting the salt intrusion zone downstream (Online Resource 6) and resulted in significantly high winter PDSi concentrations, similar to those recorded by Morris et al. (1984) in the Severn, and in the Scheldt (see Van Der Zee and Chou 2005; Van Damme et al. 2005; Arndt et al. 2009).

The Severn had relatively low riverine PDSi concentrations compared to the global average (8.3–13.1 mg/L) (see Table 4). However, the $\delta^{30}\text{Si}_{\text{DSi}}$ of the River Severn were within the range reported for 557 rivers (− 0.14 to +4.66‰) (see Table 4). The non-conservative behaviour and heavy isotopic compositions of the river waters are consistent with biological uptake by pelagic diatoms, as has been observed in other estuary systems (e.g., Zhang et al. 2020). However, the Si input from the tributaries (Usk, Wye, Avon and Cardiff Bay) and groundwater would also have influenced the spatio-temporal variation in PDSi concentrations and Si isotopic signatures. To what degree this groundwater DSi supply fuelled and controlled the Severn's DSi and isotopic budget remains unknown, advocating the need for further research into this nutrient pathway, and the influence it may have on enriching nutrient levels in coastal environments.

Pelagic BSi dynamics

Compared to PDSi, the concentration of PBSi were relatively high in the Severn Estuary (Fig. 3). Unlike other systems where PBSi is controlled by pelagic primary production, the high turbidity (Fig. 3) in the Severn Estuary reduced light availability, and likely restricted phytoplankton growth, resulting in a lack of chlorophyll fluorescence readings and low water column primary productivity. Low phytoplankton production has been observed previously in the Severn Estuary (Joint and Pomroy 1981; Underwood 2010) and other tidal-dominated estuarine systems, e.g., marine-brackish parts of the Scheldt (<0.05 chl *a* mg/L, Carbonnel et al. 2009). Despite tidal systems having long residence times (see Gao et al. 2020), the lack of pelagic production (regardless of seasonal changes) likely allowed the transport of nutrients out of the estuary preventing any significant DSi retention (calculated following Vollenweider 1968, see Online Resource 7). The lack of DSi retention contrasts with the high average values used in estimates of global Si budgets: 20% (DeMaster 1981; Tréguer and De La Rocha 2013); 25% for temperate rivers (Tréguer et al. 1995); 15% for 19 worldwide estuaries (Roubeix 2007).

High benthic productivity

Consideration of the relatively low riverine/tributary supply of PBSi, the relatively low marine PBSi concentrations and the low phytoplankton productivity, would indicate that the relatively high estuarine PBSi originated from an alternative source. Compared to the pelagic system, the benthic diatom-dominated biofilms on the intertidal mudflats had high productivity (rETR_{max} of up to 223 rel. units, Table 3) driven by their adaption to the harsh mudflat environment (see Online Resource 1), including behavioural down-regulation through cell motility away from high irradiance levels and down-regulation via the induction of non-photochemical quenching (Perkins et al. 2010). These adaptations likely allowed the diatoms to maximise photosynthetic efficiency which aided the growth of biomass-rich biofilms (116.8 µg/g *dw. sed.* Table 3), and the production of BBSi (Fig. 5).

Biologically productive, rich biofilms are also supported by the isotopically heavy mudflat waters (Fig. 6). Benthic biological activity and the

Table 4 Global river and estuary dissolved silicon and biogenic silica concentrations, and silicon isotope signatures

Location	DSi (mg/L)	DSi ($\mu\text{mol/L}$)	DSi (Mmol/yr)	BSi (mg/L)	BSi ($\mu\text{mol/L}$)	BSi (Mmol/yr)	$\delta^{30}\text{Si}$ (‰)	Study
River Severn (Winter)	2.6	89	610	0.9	47	224		Present study
River Severn (Spring)	1.4	52	112	1.3	64	105		Present study
River Severn (Summer)	3.4	112	256	0.3	14	20	+0.61 → +0.87	Present study
River Severn (Autumn)	2.6	89	109	0.5	26	19	+0.64 → +0.85	Present study
Severn Estuary (Winter)	1.5	45	182,449	0.9	53	146,700		Present study
Severn Estuary (Spring)	0.9	30	122,506	2.4	101	321,903		Present study
Severn Estuary (Summer)	1.0	30	131,437	3.4	68	311,079	+0.91 → +1.02	Present study
Severn Estuary (Autumn)	1.0	31	134,711	3.5	114	444,077	+0.93 → +1.05	Present study
Bristol Channel (Winter)	1.2	40	416,282	0.5	19	193,795		Present study
Bristol Channel (Spring)	0.8	28	225,813	2.2	75	600,314		Present study
Bristol Channel (Summer)	0.9	32	275,775	1.4	47	404,737	+1.04	Present study
Bristol Channel (Autumn)	0.8	27	266,722	1.9	67	653,680	+0.93	Present study
Scheldt River			612 ^a			148 ^b	+0.9 → 1.7 ^c	a. Carbonnel et al. (2013) b. Hughes et al. (2013) c. Frings et al. (2016)
Amazon River		138			74			Conley (1997)
Mississippi River		98			14			Conley (1997)
Danube River, Europe		55			18			Conley (1997)
Columbia River		116			37			Conley (1997)
Congo River, Africa		185			38			Conley (1997)

Table 4 (continued)

Location	DSi (mg/L)	DSi ($\mu\text{mol/L}$)	DSi (Mmol/yr)	BSi (mg/L)	BSi ($\mu\text{mol/L}$)	BSi (Mmol/yr)	$\delta^{30}\text{Si}$ (‰)	Study
Atchafalaya River, USA		113			25			Conley (1997)
Susquehanna River, USA		52			23			Conley (1997)
Connecticut River, USA		120			31			Conley (1997)
Lena River, Russia					8			Conley (1997)
Rhine River, Netherlands					23			Conley (1997)
Qiantangjiang, China	128		4,380		30.9	1,050		Li et al. (2019)
Minjiang, China	208		11,160		30.6	1,640		Li et al. (2019)
Jiulongjiang, China	261		3,050		31.7	370		Li et al. (2019)
Jiaojiang, China	162		1,080		31.3	210		Li et al. (2019)
Oujiang, China	150		2,190		31.4	460		Li et al. (2019)
Yangtze River, China	102		81,330		21	16,740		Li et al. (2019)
Yangtze Estuary, China							+0.7 → +3.4	Ding et al. (2004)
Yangtze Estuary, China							+1.70 → +2.61	Zhang et al. (2020)
Pearl River Estuary, China							+1.37 → +1.78	Zhang et al. (2020)
Amazon Estuary							+1.67 → +3.02	Zhang et al. (2020)
Nile Estuary (dry season)							+1.54 → +4.66	Cockerton et al. (2013)
Nile Estuary (wet season)							+0.48 → +3.45	Cockerton et al. (2013)
Changjiang Estuary (dry season)							+1.48 → +2.35	Zhang et al. (2015)

Table 4 (continued)

Location	DSi (mg/L)	DSi (μmol/L)	DSi (Mmol/yr)	BSi (mg/L)	BSi (μmol/L)	BSi (Mmol/yr)	$\delta^{30}\text{Si}$ (‰)	Study
Changjiang Estuary (wet season)							+ 1.54 → + 1.95	Zhang et al. (2015)
Ganges River, Himalaya							+ 0.49 → + 2.17	Frings et al. (2016)
Switzerland (40 rivers)							avg. 0.84	Georg et al. (2006)
Lake Baikal, Siberia inflow							+ 0.9 → + 1.77	Panizzo et al. (2017)
Selenga Delta							avg. + 1.52	Panizzo et al. (2017)
Congo River wetlands							+ 0.02	Cardinal et al. (2010)
Grassland surface flow	Avg. 3.5							Thieu et al. (2009)
Arable land surface flow	Avg. 3.8							Thieu et al. (2009)
Forests surface flow	3.64							Thieu et al. (2009)
Europe (and Greenland)	5.6							Dürr et al. (2011)
Africa	12.6							Dürr et al. (2011)
N. America	8							Dürr et al. (2011)
S. America	9							Dürr et al. (2011)
Asia	10							Dürr et al. (2011)
Australia	11.8							Dürr et al. (2011)
Average Global River		158 ^a	6.2 × 10 ^{6b}			1.9 × 10 ^{6c}		a. Dürr et al. (2011) b. Tréguer et al. (2021) c. Frings et al. (2016)

preferential uptake of ^{28}Si (i.e., isotopic fractionation) led to isotopically heavy residual mudflat pore-water, with values reaching highs of > 2.0‰. However, alongside the benthic biological mediation of Si, several abiotic processes could have also influenced Si concentrations and led to complex isotopic

signatures. For example: transformation of silica into clay minerals (reverse weathering); dissolution of BSi and higher plants and regeneration of DSi following deposition under specific conditions (factor of saturation state, pH, temperature); dissolution of clays (resulting in isotopically light waters); and

adsorption–desorption of DSi onto aluminium oxide surfaces of clay minerals (remove/supply DSi into the system) (Michalopoulos and Aller 1995; Weiss et al. 2015; Pickering et al. 2020).

Export of BBSi to the water column

This study supports the conclusion put forward in Welsby et al. (2016); the biofilms had fast turn-over rates, increasing the accumulation of BBSi between immersion periods. However, due to the strong hydrodynamics (Uncles 2010), with strong maximum current velocities that enhance the resuspension of the sediment and the associated diatom-dominated biofilms, the BBSi could not build-up at the SWI, resulting in low standing stocks of BBSi (< 1%). These low BBSi standing stocks are comparable to those in other estuarine systems, for example, BBSi between 0.05 and 1.5% in the Scheldt (Chou and Wollast 2006), but were slightly elevated compared to samples from the same mudflats in 2014 (Welsby et al. 2016). Importantly, due to the hypertidal characteristics of the Severn (large intertidal mudflats, strong hydrodynamics), the potential cyclic remobilisation of the biofilms could supply a continuous reservoir of BBSi to the water column (high PBSi, max. 10 mg/L, Fig. 3), which would have been subjected to the estuarine hydro-geodynamic processes of deposition, burial, and resuspension.

The calculated bottom shear stress was comparable to published critical erosion threshold values of the Severn Estuary biofilms, τ_{0cr} : 3.33 N/m² (Yallop et al. 2000). Uncles (2010) report maximum mean spring tidal (MST) current velocities of 3 m/s in the Severn Estuary, with mean neap tides (MNT) of approximately half the MST velocities. MST current velocities resulted in a bottoms shear stress of 55.2 N/m² >> 3.33–10.8 N/m², suggesting the MST currents would have easily exceeded the erosion threshold of the biofilms. Even the MNT currents, with a bottom shear stress of 13.8 N/m² > 3.33–10.8 N/m², would have led to some erosion. It is plausible that the erosion of the biofilms led to the transport of BSi to the water column on spring-neap tidal cycles, resulting in high pelagic BSi and SPM concentrations (Fig. 3).

Retention vs export of BSi in the Severn

The resuspended benthic diatoms (BSi) are typically bound by a polymer-rich biofilm formed from extracellular polymeric substances (EPS), (Yallop et al. 2000). The fast-flowing tidal currents associated with high bottom shear stress would have exceeded the erosion threshold of these biofilms despite their bio-stabilising role. In the turbulent, saline water column of the estuary the biofilms rich in organic matter and the SPM may consolidate to form one entity, known as ‘bioflocculation’ (Manning et al. 2013). These bio-flocs explain the significant linear correlation (Fig. 3) and the strong coupling between PBSi (benthic signature) and SPM (predominately mud) (Fig. 4) as BBSi and sediment originate from the intertidal mudflats and remained as one entity in the water column. Furthermore, once current velocities decrease and with bioflocculation increasing floc size and enhancing sinking velocities, SPM and PBSi concentrations in the estuarine bottom water increased (Fig. 3), contributing to BSi retention in the estuary: winter (50%), spring (2%), summer (2%) and autumn (24%) (see Online Resource 7). These estimates are in line with BSi retention values from Chesapeake Bay (65%, D’Elia et al. 1983) and the Bay of Brest (48%, Rague-neau et al. 2005). This erosion–deposition–recycling cycle makes calculating the transport of BBSi in the Severn complex, and therefore further research is required to quantify the export of BBSi to the water column in the Severn Estuary. Compared to the estimated global riverine amorphous silica (including BSi) supply of 1.9 ± 1.0 Tmol/yr in Frings et al. (2016), surprisingly the Severn Estuary accounted for approximately 16% of this budget. Therefore, the consumption and production of Si by the benthic ecosystem are significant in hypertidal estuarine systems with large intertidal mudflats like the Severn. It is acknowledged that the biogenic silica content was generally measured on thicker biofilms, and that the BBSi flux per unit area is potentially overestimated given the ‘patchy’ nature of these biofilms (Orvain et al. 2003). Regardless, these estuarine systems and their tight benthic–pelagic coupling (driven by BBSi) must be included in Si budget mass balance estimates.

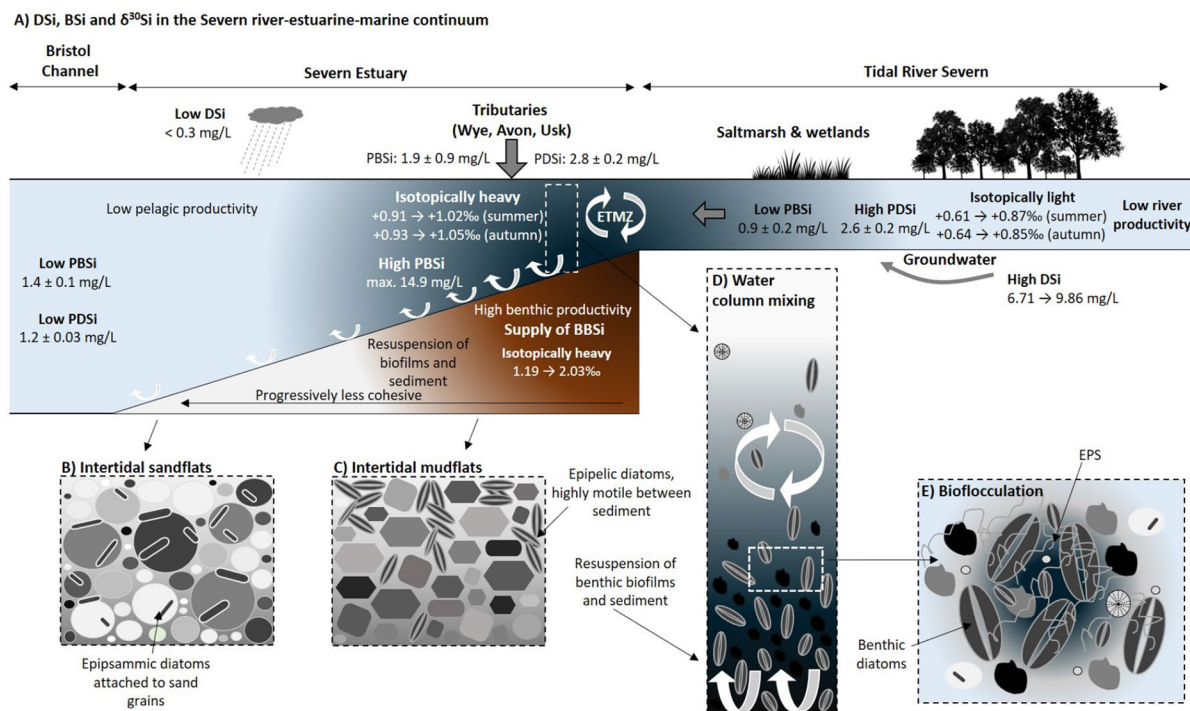


Fig. 7 Summary of dissolved silicon (DSi), biogenic silica (BSi) transport and silicon isotope signatures in the river-estuary-marine continuum of the Severn. **A** Flux of PDSi and PBSi from the River Severn and tributaries into the Severn Estuary. Benthic algal biofilm productivity—export of BBSi and $\delta^{30}\text{Si}_{\text{DSi}}$ from the intertidal mudflats into the water column of the Severn Estuary. **B** Epipsammic diatoms attached to sand

grains in the intertidal sand flats, e.g., Site 4 (Sand Bay). **C** Epipellic diatoms move freely between sediment grains in the intertidal mudflats. **D** Water column mixing. **E** Organic matter, sourced from the rivers, land run-off and re-suspended biofilms aid in the biofloculation of suspended matter. ETM zone: Estuarine Turbidity Maximum zone in the upper estuary

Si isotopes: strong benthic-pelagic cycling of Si

The Si isotopic data further supports the idea of strong benthic-pelagic cycling of Si in the Severn Estuary (Fig. 7). Coupled to the decrease in PDSi, there was a progressive and systematic downstream enrichment in heavy isotopes (Fig. 6), similar to the observations of Cockerton et al. (2013) in the Nile, Delvaux et al. (2013) in the Scheldt, and Weiss et al. (2015) in the Elbe, Germany. The resuspension of BBSi along with the mixing of isotopically enriched mudflat porewater, likely led to the isotopically heavy estuarine waters (Fig. 6). Future research on Si isotopes from mudflat settings should explore the effects of high organic carbon content, and other background matrix issues, on mass spectrometry analysis. Further, one of the key issues in estimating global $\delta^{30}\text{Si}_{\text{DSi}}$ is that they are extrapolated from riverine values, which

do not include important variations induced by the complex estuarine dynamics.

Conclusion

For the first time, a time-series dataset of Si concentrations in the Severn has been produced, which has improved our knowledge of the pelagic-benthic Si cycle in hypertidal estuaries. These findings highlight the importance of documenting the way in which an estuary modifies Si along its path to the ocean, prior to incorporating the riverine Si flux into global Si budgets. This is particularly important in benthic-dominated systems where multiple erosion-deposition cycles interfere with the riverine input signals.

Biotic and abiotic processes on the vast intertidal mudflats controlled the Severn's Si cycle. They have been shown to modify the benthic Si budgets,

together with the isotopic signatures of the mudflat water. Upon immersion, these benthic fractions and isotopic signatures are transported into the water column, preventing the build-up of BBSi despite its continuous supply by the biologically productive benthic diatoms. Once in the pelagic realm, the BSi likely undergoes a series of erosion–deposition events and can be removed from the system through burial/dissolution (retention) or can be transport out of the estuary on the tide. Here we show that the Severn Estuary has tight benthic–pelagic coupling. However, compared to other estuarine systems where this coupling is driven by pelagic production, in the Severn, the coupling is driven by benthic production (BBSi). Considering a large fraction of BSi is exported from the mudflats, and unlike DSi, could be transport further afield (DSi would likely be used up in more productive, less turbid areas of the Severn), the BSi could dissolve and replenish the Bristol Channel and even the Celtic Sea, with ‘new’ DSi ready to be consumed by phytoplankton, the latter supporting several important fisheries. Through continued field campaigns and modelling efforts, future research should investigate the transport of this benthic intertidal Si to the estuarine water column, and the transport of this estuarine-sourced BSi out to the Bristol Channel and Celtic Sea.

Acknowledgements We acknowledge the role of Ian Fryett (Cardiff University Research Vessel Skipper), and fieldwork assistants: Jen Pinnion, Dr Scott Armstrong, Dr Hong Chin Ng, Lucy Taylor, Dr Elaine Mawbey, Dr Leanne Staddon, Dr Timothy Gregory, Dr Frances Boreham, Dr Edward Bunker, James Chen and George Wallington. We acknowledge the role of laboratory assistant Jolene Cook, and members of the Bristol Isotope Group, including Dr Lucie Cassarino, Dr Jade Hatton and Dr Stephanie Bates. We acknowledge the help of Malcolm Woodward (Plymouth Marine Laboratory) for measuring nutrient concentrations. We acknowledge the help of Dr Fotis Sgouridis and the team in the School of Geographical Sciences laboratory for measuring Total Organic Carbon concentrations. We acknowledge the Environment Agency for providing nutrient, hydrology and groundwater data on the Severn Estuary to support our findings. Thanks to two anonymous reviewers, whose comments improved the manuscript.

Author contributions All authors contributed to the study conception and design. Fieldwork preparation, data collection and analysis were performed by HW. The first draft of the manuscript was written by HW and all authors commented on previous versions of the manuscript. All authors read and approved the final manuscript.

Funding This research was supported by the Tratman Scholarship at the University of Bristol.

Data availability The datasets generated during this study are available at <https://doi.org/10.5281/zenodo.7236058>. Environment Agency (EA), UK, environmental monitoring data are held under the Open Government Licence v3.0.

Declarations

Competing interest The authors have no relevant financial or non-financial interest to disclose.

Open Access This article is licensed under a Creative Commons Attribution 4.0 International License, which permits use, sharing, adaptation, distribution and reproduction in any medium or format, as long as you give appropriate credit to the original author(s) and the source, provide a link to the Creative Commons licence, and indicate if changes were made. The images or other third party material in this article are included in the article’s Creative Commons licence, unless indicated otherwise in a credit line to the material. If material is not included in the article’s Creative Commons licence and your intended use is not permitted by statutory regulation or exceeds the permitted use, you will need to obtain permission directly from the copyright holder. To view a copy of this licence, visit <http://creativecommons.org/licenses/by/4.0/>.

References

- Arndt S, Regnier P (2007) A model for the benthic–pelagic coupling of silica in estuarine ecosystems: sensitivity analysis and system scale simulation. *Biogeosci Discuss* 4(2):747–796
- Arndt S, Vanderborcht JP, Regnier P (2007) Diatom growth response to physical forcing in a macrotidal estuary: coupling hydrodynamics, sediment transport, and biogeochemistry. *J Geophys Res: Oceans*. <https://doi.org/10.1029/2006JC003581>
- Arndt S, Regnier P, Vanderborcht JP (2009) Seasonally-resolved nutrient export fluxes and filtering capacities in a macrotidal estuary. *J Mar Syst* 78(1):42–58
- Brewin RJ, de Mora L, Jackson T, Brewin TG, Shutler J (2016) Correction: on the potential of surfers to monitor environmental indicators in the coastal zone. *PLoS ONE* 11(9):e0162591
- Carbonnel V, Lionard M, Muylaert K, Chou L (2009) Dynamics of dissolved and biogenic silica in the freshwater reaches of a macrotidal estuary (The Scheldt, Belgium). *Biogeochemistry* 96(1–3):49–72
- Carbonnel V, Vanderborcht JP, Lionard M, Chou L (2013) Diatoms, silicic acid and biogenic silica dynamics along the salinity gradient of the Scheldt estuary (Belgium/The Netherlands). *Biogeochemistry* 113(1–3):657–682
- Cardinal D, Alleman LY, de Jong J, Ziegler K, André L (2003) Isotopic composition of silicon measured by multicollector plasma source mass spectrometry in dry plasma mode. *J Anal Spectrom* 18(3):213–218

- Cardinal D, Gaillardet J, Hughes HJ, Opfergelt S, André L (2010) Contrasting silicon isotope signatures in rivers from the Congo basin and the specific behaviour of organic-rich waters. *Geophys Res Lett.* <https://doi.org/10.1029/2010GL043413>
- Carey J, Fulweiler R (2014) Salt marsh tidal exchange increases residence time of silica in estuaries. *Limnol Oceanogr* 59(4):1203–1212
- Chou L, Wollast R (2006) Estuarine silicon dynamics. In: Ittekkot D, Unger C, Humborg C, TacAn N (eds) *The silicon cycle: human perturbations and impacts on aquatic systems*. Scope, pp 93–120
- Chou L, Carbonnel V, Vanderborcht JP, Røevros N, Tsagaris M, Zeeder VC, Leonard M, Muylaert K, Dasseville R, Viverman W (2007) Silica retention in the Scheldt continuum and its impact on coastal eutrophication (SISCO). Final report EV/17. Belgian Science Policy, Brussel, p 95
- Cockerton H, Street-Perrott F, Leng M, Barker P, Horstwood M, Pashley V (2013) Stable-isotope (H, O, and Si) evidence for seasonal variations in hydrology and Si cycling from modern waters in the Nile Basin: implications for interpreting the Quaternary record. *Quatern Sci Rev* 66:4–21
- Conley DJ (1997) Riverine contribution of biogenic silica to the oceanic silica budget. *Limnol Oceanogr* 42(4):774–777
- Conley DJ, Malone TC (1992) Annual cycle of dissolved silicate in Chesapeake bay: implications for the production and fate of phytoplankton biomass. *Marine ecology progress series*. Oldendorf 81(2):121–128
- D'Elia CF, Nelson DM, Boynton WR (1983) Chesapeake bay nutrient and plankton dynamics: III. The annual cycle of dissolved silicon. *Geochim Et Cosmochim Acta* 47(11):1945–1955
- Delvaux C, Cardinal D, Carbonnel V, Chou L, Hughes H, André L (2013) Controls on riverine $\delta^{30}\text{Si}$ signatures in a temperate watershed under high anthropogenic pressure (Scheldt Belgium). *J Mar Syst* 128:40–51
- DeMaster DJ (1981) The supply and accumulation of silica in the marine environment. *Geochim Cosmochim Acta* 45(10):1715–1732
- Ding T, Wan D, Wang C, Zhang F (2004) Silicon isotope compositions of dissolved silicon and suspended matter in the Yangtze River. *China Geochim Et Cosmochim Acta* 68(2):205–216
- Dürr HH, Meybeck M, Hartmann J, Laruelle GG, Roubeix V (2011) Global spatial distribution of natural riverine silica inputs to the coastal zone. *Biogeosciences* 8(3):597–620
- Environment Agency (EA), 2016. Hydrology and nutrient data. Supplied upon request in 2019
- Environment Agency (EA), 2017. Southwest groundwater Si data. Supplied upon request in 2017
- Frings PJ, Clymans W, Fontorbe G, Christina L, Conley DJ (2016) The continental Si cycle and its impact on the ocean Si isotope budget. *Chem Geol* 425:12–36
- Gao G, Xia J, Falconer R, Wang Y (2020) Modelling study of transport time scales for a hyper-tidal estuary. *Water* 12:2434. <https://doi.org/10.3390/w12092434>
- Georg R, Reynolds BC, Frank M, Halliday AN (2006) Mechanisms controlling the silicon isotopic compositions of river waters. *Earth Planet Sci Lett* 249(3–4):290–306
- Hendry KR, Leng MJ, Robinson LF, Sloane HJ, Blusztjan J, Rickaby RE, Georg RB, Halliday AN (2011) Silicon isotopes in Antarctic sponges: an interlaboratory comparison. *Antarct Sci* 23(1):34–42
- Hughes HJ, Delvigne C, Korntheuer M, De Jong J, André L, Cardinal D (2011) Controlling the mass bias introduced by anionic and organic matrices in silicon isotopic measurements by MC-ICP-MS. *J Anal At Spectrom* 26(9):1892–1896
- Hughes HJ, Sondag F, Santos RV, André L, Cardinal D (2013) The riverine silicon isotope composition of the amazon basin. *Geochim Cosmochim Acta* 121:637–651
- Hydes, D., Aoyama, M., Aminot, A., Bakker, K., Becker, S., Coverly, S., Daniel, A., Dickson, A., Grosso, O., Kerouel, R., et al. (2010). Determination of Dissolved Nutrients (N, P, Si) in Seawater With High Precision and Inter-Comparability Using Gas-Segmented Continuous Flow Analysers
- Jacobs S, Struyf E, Maris T, Meire P (2008) Spatiotemporal aspects of silica buffering in restored tidal marshes. *Estuar Coast Shelf Sci* 80(1):42–52
- Joint I, Pomroy A (1981) Primary production in a turbid estuary. *Estuar Coast Shelf Sci* 13(3):303–316
- Karl DM, Tien G (1992) MAGIC: a sensitive and precise method for measuring dissolved phosphorus in aquatic environments. *Limnol Oceanogr* 37(1):105–116
- Leynaert A, Longphuirt SN, An S, Lim J-H, Clauquin P, Grall J, Kwon BO, Koh CH (2011) Tidal variability in benthic silicic acid fluxes and microphytobenthos uptake in intertidal sediment. *Estuar Coast Shelf Sci* 95(1):59–66
- Li D, Dong M, Liu S, Chen H, Yao Q (2019) Distribution and budget of biogenic silica in the Yangtze estuary and its adjacent sea. *Sci Total Environ* 669:590–599
- Mackereth F, Heron J, Talling J (1978) Water analysis of freshwater. *Biol Ass Publ* 36:120
- Manning A, Langston W, Jonas P (2010) A review of sediment dynamics in the Severn estuary: influence of flocculation. *Mar Pollut Bull* 61(1–3):37–51
- Manning AJ, Spearman JR, Whitehouse RJ, Pidduck EL, Baugh JV, Spencer KL (2013) Flocculation dynamics of mud: sand mixed suspensions. Sediment transport processes and their modelling applications. IntechOpen, London
- Michalopoulos P, Aller RC (1995) Rapid clay mineral formation in amazon delta sediments: reverse weathering and oceanic elemental cycles. *Science* 270(5236):614–617
- Morris A (1984) The chemistry of the Severn estuary and the Bristol channel. *Mar Pollut Bull* 15(2):57–61
- Neill, S. P. and Couch, S. J. (2011). Impact of Tidal Energy Converter (TEC) array operation on sediment dynamics. In Proceedings of the 9th European Wave and Tidal Energy Conference
- Met Office (2016). Historical Station Observations. <https://www.metoffice.gov.uk/research/climate/maps-and-data/historic-station-data> [Accessed 20/10/22]
- Orvain F, Galois R, Barnard C, Sylvestre A, Blanchard G, Sauriau PG (2003) Carbohydrate production in relation to microphytobenthic biofilm development: an integrated approach in a tidal mesocosm. *Microb Ecol* 45(3):237–251

- Panizzo VN, Swann GE, Mackay AW, Vologina E, Alleman L, André L, Horstwood MS (2017) Constraining modern-day silicon cycling in Lake Baikal. *Global Biogeochem Cycles* 31(3):556–574
- Pastuszek M, Conley DJ, Humborg C, Witek Z, Sitek S (2008) Silicon dynamics in the Oder estuary, Baltic Sea. *J Mar Syst* 3(73):250–262
- Paterson DM (1989) Short-term changes in the erodibility of intertidal cohesive sediments related to the migratory behavior of epipelagic diatoms. *Limnol Oceanogr* 34(1):223–234
- Perkins RG, Paterson DM, Sun H, Watson J, Player MA (2004) Extracellular polymeric substances: quantification and use in erosion experiments. *Cont Shelf Res* 24(15):1623–1635
- Perkins RG, Lavaud J, Serôdio J, Mouget J-L, Cartaxana P, Rosa P, Barillé L, Brotas V, Jesus BM (2010) Vertical cell movement is a primary response of intertidal benthic biofilms to increasing light dose. *Mar Ecol Prog Ser* 416:93–103
- Pickering RA, Cassarino L, Hendry KR, Wang XL, Maiti K, Krause JW (2020) Using stable isotopes to disentangle marine sedimentary signals in reactive silicon pools. *Geophys Res Lett* 47(15):e2020GL087877
- Ragueneau O, Chauvaud L, Moriceau B, Leynaert A, Thouzeau G, Donval A, Le Loch F, Jean F (2005) Biodeposition by an invasive suspension feeder impacts the biogeochemical cycle of Si in a coastal ecosystem (Bay of Brest, France). *Biogeochemistry* 75(1):19–41
- Raimonet M, Ragueneau O, Andrieux-Loyer F, Philippon X, Kérouel R, Le Goff M, Mémerly L (2013) Spatio-temporal variability in benthic silica cycling in two macrotidal estuaries: causes and consequences for local to global studies. *Estuar Coast Shelf Sci* 119:31–43
- Regnier P, Arndt S, Goossens N, Volta C, Laruelle GG, Lauerwald R, Hartmann J (2013) Modelling estuarine biogeochemical dynamics: from the local to the global scale. *Aquat Geochem* 19(5–6):591–626
- Reynolds BC, Frank M, Halliday AN (2006) Silicon isotope fractionation during nutrient utilization in the North Pacific. *Earth Planet Sci Lett* 244(1–2):431–443
- Roubeix, V. (2007). Transformations biogochimiques et transfert du silicium dans la zone de transition fleuve-mer: le rôle des diatomées planctoniques. PhD thesis, Université Libre de Bruxelles, Belgium
- Sarath PK, Mangalaa KR, Cardinal D, Gurumurthy GP, Dapoigny A, Sarma VVSS, Riotte J (2022) Seasonal, weathering and water use controls of silicon cycling along the river flow in two contrasting basins of South India. *Chem Geol*. <https://doi.org/10.1016/j.chemgeo.2022.120883>
- Stal L, De Brouwer J (2003) Biofilm formation by benthic diatoms and their influence on the stabilization of intertidal mudflats. *Berichte-Forschungszentrum Ter-Ramare* 12:109–111
- Strickland, J. D. and Parsons, T. R. (1972). A practical handbook of seawater analysis
- Struyf E, Van Damme S, Gribsholt B, Meire P (2005a) Freshwater marshes as dissolved silica recyclers in an estuarine environment (Schelde estuary, Belgium). *Hydrobiologia* 540(1–3):69
- Struyf E, Van Damme S, Gribsholt B, Middelburg JJ, Meire P (2005b) Biogenic silica in tidal freshwater marsh sediments and vegetation (Schelde estuary, Belgium). *Mar Ecol Prog Ser* 303:51–60
- Struyf E, Mörth C-M, Humborg C, Conley DJ (2010) An enormous amorphous silica stock in boreal wetlands. *J Geophys Res: Biogeosci*. <https://doi.org/10.1029/2010JG001324>
- Sutherland T, Amos C, Grant J (1998) The effect of buoyant biofilms on the erodibility of sublittoral sediments of a temperate microtidal estuary. *Limnol Oceanogr* 3(2):225–235
- Thieu V, Billen G, Garnier J (2009) Nutrient transfer in three contrasting NW European watersheds: the Seine, Somme, and Scheldt Rivers. A comparative application of the Seneque/Riverstrahler model. *Water Res* 43(6):1740–1754
- Tréguer PJ, De La Rocha CL (2013) The world ocean silica cycle. *Ann Rev Mar Sci* 5:477–501
- Tréguer P, Nelson DM, Van Bennekom AJ, DeMaster DJ, Leynaert A, Queguiner B (1995) The silica balance in the world ocean: a re-estimate. *Science* 268(5209):375–379
- Tréguer P, Bowler C, Moriceau B, Dutkiewicz S, Gehlen M, Aumont O, Pondaven P (2018) Influence of diatom diversity on the ocean biological carbon pump. *Nat Geosci* 11(1):27–37
- Tréguer PJ, Sutton JN, Brzezinski M, Charette MA, Devries T, Dutkiewicz S, Rouxel O (2021) Reviews and syntheses: The biogeochemical cycle of silicon in the modern ocean. *Biogeosciences* 18(4):1269–1289
- Uncles R (2010) Physical properties and processes in the Bristol channel and Severn estuary. *Mar Pollut Bull* 61(1–3):5–20
- Underwood GJ (2010) Microphytobenthos and phytoplankton in the Severn estuary, UK: present situation and possible consequences of a tidal energy barrage. *Mar Pollut Bull* 61(1–3):83–91
- Underwood GJC, Paterson DM (1993) Seasonal changes in diatom biomass, sediment stability and biogenic stabilization in the Severn estuary. *J Mar Biol Assoc UK* 73(4):871–887
- Van Damme S, Struyf E, Maris T, Ysebaert T, Dehaers F, Tackx M, Heip C, Meire P (2005) Spatial and temporal patterns of water quality along the estuarine salinity gradient of the Scheldt estuary (Belgium and The Netherlands): results of an integrated monitoring approach. *Hydrobiologia* 540(1–3):29–45
- Van Der Zee C, Chou L (2005) Seasonal cycling of phosphorus in the Southern Bight of the North Sea. *Biogeosciences* 2(1):27–42
- Visco G, Campanella L, Nobili V (2005) Organic carbons and TOC in waters: an overview of the international norm for its measurements. *Microchem J* 79(1–2):185–191
- Vollenweider, R. (1968). Scientific fundamentals of the eutrophication of lakes and flowing waters, with particular reference to phosphorus and nitrogen as factors in eutrophication. *Organ. Econ. Coop. Devel. Tech. Rep. OAS/CSI/68.27*
- Volta C, Arndt S, Savenije HH, Laruelle GG, Regnier P (2014) C-GEM (v 10): a new, cost-efficient biogeochemical model for estuaries and its application to a funnel-shaped system. *Geosci Model Dev* 7(4):1271–1295
- Weiss A, De La Rocha C, Amann T, Hartmann J (2015) Silicon isotope composition of dissolved silica in surface waters of the Elbe Estuary and its tidal marshes. *Biogeochemistry* 124(1–3):61–79

- Welsby H, Hendry K, Perkins R (2016) The role of benthic biofilm production in the mediation of silicon cycling in the Severn Estuary, UK. *Estuar Coast Shelf Sci* 176:124–134
- Yallop M, Paterson D, Wellsbury P (2000) Interrelationships between rates of microbial production, exopolymer production, microbial biomass, and sediment stability in biofilms of intertidal sediments. *Microb Ecol* 39(2):116–127
- Zhang A, Zhang J, Hu J, Zhang R, Zhang G (2015) Silicon isotopic chemistry in the Changjiang Estuary and coastal regions: impacts of physical and biogeochemical processes on the transport of riverine dissolved silica. *J Geophys Res: Oceans* 120(10):6943–6957
- Zhang Z, Cao Z, Grasse P, Dai M, Gao L, Kuhnert H, Frank M (2020) Dissolved silicon isotope dynamics in large river estuaries. *Geochim Cosmochim Acta* 273:367–382

Publisher's Note Springer Nature remains neutral with regard to jurisdictional claims in published maps and institutional affiliations.